Respiration rate modeling of Cavendish banana (*Musa acuminata* cv. Cavendish) under various storage temperatures

Dimas Triardianto[1*], *Yani* Subaktillah[1], *A. Sirojul Anam Izza* Rosyadi[1], *Annisa'U* Choirun[1], and Shinta *Widyaningtyas*[1]

[1]Departement of Agricultural Technology, Politeknik Negeri Jember, Jember, Indonesia

Abstract. Cavendish banana (Musa acuminata cv. Cavendish) is a climacteric fruit that is widely consumed worldwide due to its desirable sensory qualities and year-round availability. As a climacteric fruit, it exhibits a characteristically high respiration rate, which accelerates metabolic activity and results in a relatively short shelf life during postharvest handling and distribution. One of the most effective approaches to prolong shelf life is by reducing the respiration rate through low-temperature storage . This study aimed to mathematically model the respiration rate of Cavendish bananas using both the Arrhenius and Michaelis–Menten approaches to better understand the temperature dependence of respiration behavior. The samples were stored at three temperatures: 7, 17, and 27 °C (ambient). Respiration rates were monitored in a closed system at three-hour intervals over a period of three weeks. The results showed that the Arrhenius model effectively described both O_2 consumption and CO_2 production rates, supported by validation tests where the correlation coefficients (R^2) were close to one and the Chi-Square p-values exceeded 0.05. Moreover, Michaelis–Menten modeling indicated that a combination of Competitive and Uncompetitive inhibition models provided the best fit compared with other kinetic types. Validation further demonstrated consistently high R^2 values, Chi-Square p-values greater than 0.05, and low SSE and RMSE values for all samples.

1 Introduction

Bananas are among the most widely produced and traded fruits worldwide, with over 1,000 varieties contributing essential nutrients across producing and importing countries. The Cavendish dominates global trade, accounting for nearly half of total production at approximately 50 million tonnes annually. In many low-income, food-deficit nations, Cavendish bananas are particularly significant as both a staple food supporting household nutrition and a cash crop generating income [1]. Nevertheless, the shelf life of cavendish bananas is relatively short, and their climacteric behavior accelerates deterioration throughout the ripening process [2].

*Corresponding author: dimas.triardianto@polije.ac.id

As a climacteric fruit, the Cavendish banana continues to ripen after harvest, a process characterized by a respiratory climacteric peak. Once this peak is reached, the fruit enters senescence, leading to quality deterioration. Numerous studies have investigated the timing of this peak and explored strategies to delay it, with storage temperature adjustment shown to effectively slow the process and preserve fruit quality for longer periods [3].

Modeling respiration rate as a function of preservation temperature provides an effective approach to evaluate the respiratory kinetics of storage systems [4]. Several researchers have developed models to predict the respiration rate of fruits under various storage conditions. The Arrhenius equation is widely employed to model respiration rate as a function of temperature, where the activation energy (Ea) represents the minimum energy required for a reaction to occur, and lower Ea values indicate faster reaction rates with reported values for fruits [5]. In addition, the Michaelis–Menten (MM) equation has been applied to describe the relationship between enzyme kinetics and the resulting of carbon dioxide (CO_2) gas concentration from fruits respiration reaction [6,7], and has demonstrated a good fit with experimental data [8,9,10].

Specific studies on modeling the respiration rate of Cavendish bananas under three different storage temperatures have not yet been conducted. Therefore, this study aims to develop respiration rate models for Cavendish bananas stored at 7, 17, and 27 °C (ambient temperature) using the Arrhenius and Michaelis–Menten model. The resulting models are expected to provide useful insights for evaluating post-harvest quality, optimizing storage strategies, extending shelf life, and improving postharvest management of cavendish bananas.

2 Materials and Methods

2.1 Material

The experimental material consisted of freshly harvested cavendish bananas at the light-green maturity stage. Samples were selected through visual inspection to ensure the absence of disease symptoms, after which their mass and volume were measured (Table 1). The samples were then divided into three groups and stored at three different temperature conditions. Finally, each sample was placed in a respiration rate measurement system (one sample per system) and monitored for three weeks.

Table 1. Mass and Volume of The Samples

Storage Temperature (ºC)	Parameters	Cavendish Banana
7ºC	Weight (gr)	254.196 ± 0.010
	Volume (mL)	276.667 ± 0.001
17 ºC	Weight (gr)	238.970 ± 0.026
	Volume (mL)	263.333 ± 0.001
27 ºC (ambient temperature)	Weight (gr)	232.993 ± 0.008
	Volume (mL)	263.333 ± 0.001

2.2 Methods

2.2.1 Respiration Rate Measurement

The respiration rate of the samples was measured using a closed-type respiration measurement device (Figure 1). This instrument is equipped with an gas sensor capable of detecting O_2 and CO_2 during the respiration process and directly converting the measured gas concentration (%) into respiration rate values (10^{-6} $m^3/kg \cdot h$) using Equation 1 - 2. Both

CO_2 concentration and respiration rate values were displayed on an integrated LCD panel. Respiration rate measurements were recorded every 3 hours throughout the 21-day storage period.

$$R_{O_2} = \frac{\left(y_{O_2}^{ti} - y_{O_2}^{tf}\right) . V}{100 \, . \, M . \left(t_f - t_i\right)} \qquad (1)$$

$$R_{CO_2} = \frac{\left(y_{CO_2}^{tf} - y_{CO_2}^{ti}\right) . V}{100 \, . \, M . \left(t_f - t_i\right)} \qquad (2)$$

where, RO_2 represents the respiration rate in mL $(O_2)\cdot kg^{-1}\cdot h^{-1}$, RCO_2 represents the respiration rate in mL $(CO_2)\cdot kg^{-1}\cdot h^{-1}$, y is the gas concentration expressed as a percentage, Vf denotes the free volume of the respirometer in mL, M is the mass of the sample inside the chamber in kg, and ti and tf indicate the initial and final times of the measurement interval in hours.

Fig. 1. Closed-System Respirometer

2.2.2 Arrhenius Model

The Arrhenius model was applied to evaluate the effect of storage temperature on the rate of quality parameter changes under different storage conditions. This equation provides a fundamental description of the relationship between activation energy and reaction rate. The Arrhenius equation is presented in Equation 2 [11].

$$k = A \, . \, e^{-\frac{Ea}{R.T}} \qquad (3)$$

The parameters used in the Arrhenius equation are defined as follows: A represents the frequency factor, Ea denotes the activation energy $(J\cdot mol^{-1})$, R is the universal gas constant $(8.314\ J\cdot mol^{-1}\cdot K^{-1})$, and T refers to the storage temperature expressed in Kelvin (K).

2.2.3 Michaelis – Menten Model

The Michaelis–Menten model takes the form of an equation that describes the rate of enzymatic reactions by relating the reaction rate to substrate concentration. In this study, the Michaelis–Menten model was applied using five different models.

Model 1. (Simple Model) This model (Equation 4) assuming the absence of CO_2 inhibition during the respiration process, the reaction can be described using the simplified Michaelis–Menten equation [8].

$$R_{O_2/CO_2} = \frac{\alpha . Y_{O_2/CO_2}}{\phi + Y_{O_2/CO_2}} \qquad (4)$$

Model 2. (Competitive Model) The model (Equation 5) with competitive inhibition accounts for the role of CO_2 as an inhibitor in the respiration process, where both the inhibitor and the substrate (O_2) compete for binding at the same active site of the enzyme [12]. The corresponding equation is used to represent the competitive type of Michaelis–Menten kinetics.

$$R = \frac{\alpha . Y_{O_2}}{\phi\left(1+\frac{Y_{CO_2}}{\gamma_c}\right)+Y_{O_2}} \qquad (5)$$

Model 3. (Uncompetitive Model) The equation (Equation 6) with uncompetitive inhibition, in which CO_2 interacts with the enzyme–substrate complex [13].

$$R = \frac{\alpha . Y_{O_2}}{\phi + Y_{O_2}\left(1+\frac{Y_{CO_2}}{\gamma_u}\right)} \qquad (6)$$

Model 4. (Non Competitive) The Michaelis–Menten equation with non-competitive (Equation 7) inhibition describes a condition where CO_2 binds to an allosteric site, reducing the maximum reaction velocity (Vmax) without affecting the Michaelis constant [14].

$$R = \frac{\alpha . Y_{O_2}}{(\phi + Y_{O_2})\left(1+\frac{Y_{CO_2}}{\gamma_n}\right)} \qquad (7)$$

Model 5. (Combination *Competitive* and *Uncompetitive)* The CO_2 inhibition may occur simultaneously through both competitive and uncompetitive mechanisms, a process described by the following equation and referred to as the Michaelis–Menten combination inhibition model (Equation 8) [8].

$$R = \frac{\alpha . Y_{O_2}}{\phi\left(1+\frac{Y_{CO_2}}{\gamma_c}\right)+Y_{O_2}\left(1+\frac{Y_{CO_2}}{\gamma_u}\right)} \qquad (8)$$

Where, α represents the maximum rate of O_2 consumption or CO_2 production (mL O_2/kg·h; mL CO_2/kg·h). The term Φ denotes the dissociation constant of the enzyme–substrate complex, corresponding to the substrate concentration at which the respiration rate reaches half of its maximum value (%). Meanwhile, γ\gammaγ refers to the Michaelis–Menten dissociation constant, also expressed as a percentage

2.2.4 Data Analysis and Model Evaluation

The respiration rate values of all samples stored under three different temperature conditions were analyzed using one-way ANOVA. Duncan's Multiple Range Test (DMRT) was then applied to assess the effect of storage temperature and to identify significant differences among the means.

The predicted RO_2 and RCO_2 values for each sample under the different model types were evaluated using the coefficient of determination (R^2), the p-value from the Chi-square (χ^2) test, the Sum of Squares Error (SSE), and the Root Mean Square Error (RMSE), as defined by Equations (9–12). A model was considered to have good

performance when the R^2 value was high (close to 1), the p-value from the Chi-square test exceeded 0.05, and both SSE and RMSE values were low (approaching 0) [15, 16].

$$R^2 = 1 - \frac{\sum(x_{pred,i} - x_{exp,i})^2}{\sum_{i=1}^{N}(x_{pred,i} - x_{exp,i})^2} \quad (9)$$

$$X^2 = \frac{\sum_{i=1}^{N}(x_{exp,i} - x_{pre,i})^2}{N-z} \quad (10)$$

$$SSE = \frac{1}{N}\sum_{i=1}^{N}(x_{exp,i} - x_{pre,i})^2 \quad (11)$$

$$RMSE = \left[\frac{1}{N}\sum_{i=1}^{N}\left(x_{exp,i} - x_{pre,i}\right)^2\right]^{\frac{1}{2}} \quad (12)$$

Where, X_{exp} represents the experimental data of RO_2 and RCO_2, X_{pred} the predicted data of RO_2 and RCO_2, N the number of observations, and z the number of constants.

3 Results and Discussion

3.1 Changes in O_2 and CO_2 Concentrations and Respiration Rate

Changes in O_2 and CO_2 concentrations during storage are shown in Figure 2. The O_2 concentration gradually decreased throughout the storage period, while CO_2 concentration increased, reflecting the respiration process in Cavendish bananas, where O_2 is consumed, and CO_2 is produced. As illustrated in Figure 3, higher storage temperatures markedly accelerated both RO_2 and RCO_2 respiration rates. At storage temperatures of 7, 17, and 27 °C, the peak respiration rates were 12.06, 23.33, and 51.59 mL/kg·h, respectively, demonstrating a trend in which the respiration rate approximately doubled with every 10 °C increase in temperature [17]. Consistent findings were obtained by Kasim et al. [18], who observed that bananas stored at 27 °C exhibited the highest respiration rate compared with those stored at 17.5 °C and 10 °C. Although lower temperatures effectively reduce the respiration rate, excessively low storage temperatures may trigger chilling injury in bananas, which can negatively affect their texture, color, and overall postharvest quality [2].

The one-way ANOVA analysis confirmed a significant effect of storage temperature on the respiration rate of Cavendish bananas. Furthermore, the DMRT test revealed that the mean respiration rates of RO_2 and RCO_2 during storage differed significantly across all samples, as presented in Table 2.

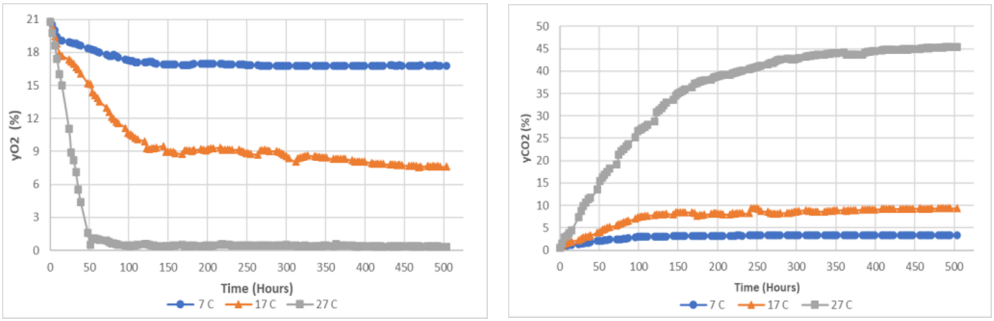

Fig. 2. Changes in O_2 and CO_2 Concentrations During Storage

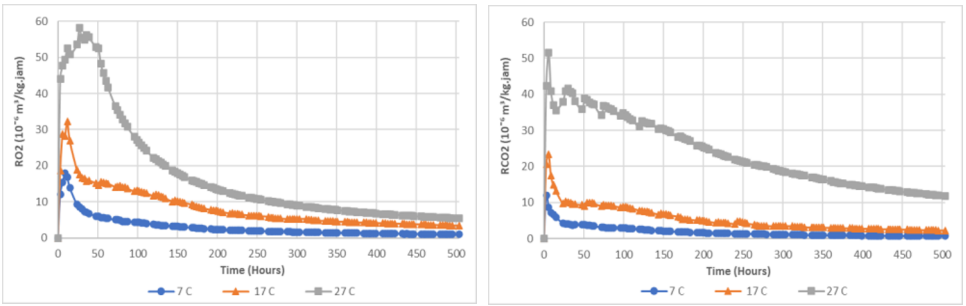

Fig. 3. Respiration Rate of Cavendish Bananas at Different Storage Temperatures

Table 2. Results of the DMRT Test on Mean Respiration Rates at Different Storage Temperatures

Parameters	Storage Temperatures (°C)		
	7	17	27
RO_2 (ml/Kg.jam)	4,62[a]	11,52[b]	17,24[c]
RCO_2 (ml/Kg.jam)	3,46[a]	9,37[b]	13,86[c]

3.2 Arrhenius Model and Evaluation

In this study, the Arrhenius model was applied to evaluate the effect of temperature on reaction kinetics, allowing the determination of both the activation energy (Ea) and the frequency factor (A). The activation energy represents the minimum energy required to initiate a reaction, with higher Ea values indicating slower reaction rates due to the greater energy barrier to reach the transition state. In addition, the frequency factor reflects the frequency of effective molecular collisions that can potentially lead to a reaction [18].

The Arrhenius modeling results for respiration rate parameters (RO_2 and RCO_2) are presented in Table 3 and Figure 4. Overall, the obtained Ea values fall within the typical activation energy range for respiration rates of fruits and vegetables, which generally lies between 29 and 92.9 kJ/mol under normal atmospheric conditions [5].

Table 3. Arrhenius model results for the respiration rates of Cavendish Banana at Different Storage Temperatures

Parameters	Ea (kJ/Mol)	A (mL/kg.jam)	Arrhennius Equation Prediction
RO2	54.67	40436553401.25	$RO2 = 40436553401.25 . e^{\frac{6576,30}{T}}$
RCO2	87.25	32564528237223900	$RCO2 = 32564528237223900 . e^{\frac{10494}{T}}$

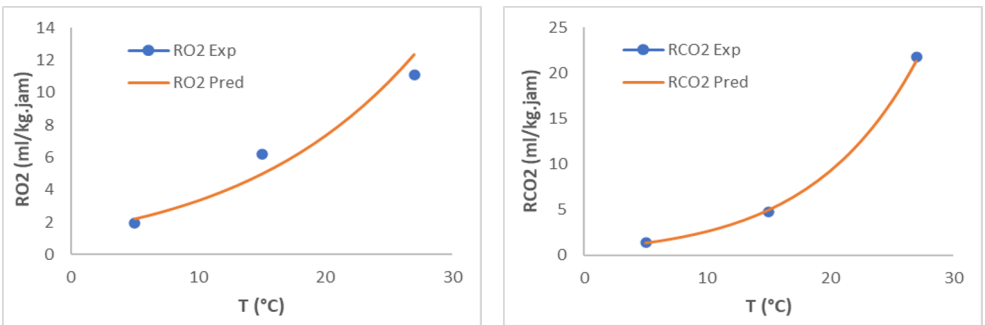

Fig. 4. Comparison of Experimental and Predicted Respiration Rates

The predicted respiration rates of RO_2 and RCO_2 were subsequently validated to assess the performance of the developed model. The validation of the Arrhenius model was conducted using two statistical methods: the correlation coefficisent (R^2) and the p-value of the Chi-square (χ^2) test. The results of the validation are presented in Table 4.

Table 4. Validation Test Results of Arrhenius Respiration Rate Modeling

Parameters	R^2	P *value* X^2
RO2	0,925	0,805
RCO2	0,999	0,989

Across all parameters, the correlation coefficients (R^2) were close to 1, while the p-values of the Chi-square (χ^2) test exceeded 0.05. These findings indicate that the Arrhenius model provides a reliable representation of the respiration rates (RO_2 and RCO_2) of Cavendish bananas during storage.

3.3 Michaelis–Menten Model and Evaluation

The parameters of the Michaelis–Menten model are presented in Table 5 - 6. The parameter values varied across storage temperatures, reflecting differences in enzymatic interactions. Lower φ values indicated a stronger affinity of the substrate (O_2) for the enzyme, suggesting that O_2 played a significant role in influencing respiration rate. In contrast, higher dissociation constants implied a greater likelihood of enzyme interaction with CO_2 [18]. The estimated parameters were subsequently applied to construct Michaelis–Menten models and to calculate the predicted respiration rates.

Table 5. Michaelis–Menten Model for RO_2

MM Model	Parameters	RO_2		
		Storage Temperature (°C)		
		7	17	27
Simple	α	-0.756	238.095	47.170
	φ	-20.545	195.214	-1.354
	Equation	$RO_2 = \frac{(-0{,}756)\,.\,YO_2}{YO_2 - (-20{,}545)}$	$RO_2 = \frac{(238{,}095)\,.\,YO_2}{YO_2 - (195{,}214)}$	$RO_2 = \frac{(47{,}170)\,.\,YO_2}{YO_2 - (-1{,}354)}$
Competitive	α	1.76	18.06	52.15
	ϕ	-21.09	-4.61	-0.26
	γc	-0.08	-3.92	-197.12
	Equation	$RO_2 = \frac{(1{,}760)\,.YO_2}{-21{,}090\,.\left(1+\frac{YCO_2}{-0{,}080}\right)+YO_2}$	$RO_2 = \frac{(-83{,}260)\,.YO_2}{-94{,}250\,.\left(1+\frac{YCO_2}{0{,}880}\right)+YO_2}$	$RO_2 = \frac{(50{,}660)\,.YO_2}{-0{,}200\,.\left(1+\frac{YCO_2}{-256{,}09}\right)+YO_2}$
Uncompetitive	α	1.86	18.06	46.09
	ϕ	-21.89	-4.61	0.65
	γc	-0.09	-3.92	70.64
	Equation	$RO_2 = \frac{(1{,}865)\,.YO_2}{21{,}890+\left(1+\frac{YCO_2}{0{,}085}\right).\,YO_2}$	$RO_2 = \frac{(18{,}064)\,.YO_2}{4{,}613+\left(1+\frac{YCO_2}{3{,}916}\right).\,YO_2}$	$RO_2 = \frac{(59{,}783)\,.YO_2}{0{,}222+\left(1+\frac{YCO_2}{269{,}844}\right).\,YO_2}$
Noncompetitive	α	2.060343	20.12061	46.61372
	ϕ	-22.6885	-3.79523	0.215571
	γc	2.004	33.366	-46.181
	Equation	$RO_2 = \frac{(2{,}060)\,.YO_2}{(YO_2-(22{,}688))\,.\left(1-\frac{YCO_2}{(2{,}004)}\right).}$	$RO_2 = \frac{(20{,}121)\,.YO_2}{(YO_2-(3{,}795))\,.\left(1-\frac{YCO_2}{(33{,}366)}\right).}$	$RO_2 = \frac{(46{,}614)\,.YO_2}{(YO_2-(0{,}216))\,.\left(1-\frac{YCO_2}{(-46{,}181)}\right).}$
Combination	α	2.060343	20.12061	46.61372
	ϕ	-22.6885	-3.79523	0.215571
	γc	5.861957	-3.28119	15.21274
	γu	2.003592	33.36649	-46.1807
	Equation	$RO_2 = \frac{(2{,}060)\,.YO_2}{(-22{,}688).\,\left(1-\frac{YCO_2}{5{,}861}\right)+YO_2\left(1-\frac{YCO_2}{(2{,}003)}\right).}$	$RO_2 = \frac{(-60{,}254)\,.YO_2}{(-65{,}183)\,.\,\left(1-\frac{YCO_2}{-23{,}824}\right)+YO_2\left(1-\frac{YCO_2}{(-4{,}240)}\right).}$	$RO_2 = \frac{(51{,}795)\,.YO_2}{(-0{,}140)\,.\,\left(1-\frac{YCO_2}{-9{,}506}\right)+YO_2\left(1-\frac{YCO_2}{(81{,}618)}\right)}$

Figure 5–6 presents a comparison between the experimental respiration rates (RO_2 and RCO_2) and those predicted by the Michaelis–Menten model. The predicted values were further evaluated using R^2, SSE, RMSE, and x^2 to determine the best fit with the experimental data (Table 7). The evaluation showed that the most suitable model varied across storage temperatures, with the Michaelis–Menten combination competitive–uncompetitive model exhibiting the highest level of agreement. This was evidenced by its consistently higher R^2 and x^2 values and lower SSE and RMSE compared with the other four models.

Table 6. Michaelis–Menten Model for RCO_2

MM Model	Parameters	RCO_2 Storage Temperature (°C)		
		7	17	27
Simple	α	1.969	7.880	33.003
	φ	-0.872	-0.745	-0.597
	Equation	$RCO_2 = \frac{(1{,}969).YCO_2}{YCO_2-(-0{,}872)}$	$RCO_2 = \frac{(7{,}880).YCO_2}{YCO_2-(-0{,}745)}$	$RCO_2 = \frac{(33{,}003).YCO_2}{YCO_2-(-0{,}597)}$
Competitive	α	-0.59	-4.04	40.01
	φ	-21,66	-27.07	0.02
	γc	0.027	0.149	1630.912
	Equation	$RCO_2 = \frac{(-0{,}590).YO_2}{-21{,}664.\left(1+\frac{YCO_2}{0{,}027}\right)+YO_2}$	$RCO_2 = \frac{(-2{,}830).YO_2}{-25{,}340.\left(1+\frac{YCO_2}{0{,}112}\right)+YO_2}$	$RCO_2 = \frac{(40{,}010).YO_2}{0{,}020.\left(1+\frac{YCO_2}{1630{,}912}\right)+YO_2}$
Uncompetitive	α	-0.68	-4.04	43.19
	φ	-21.62	-27.07	0.00
	γc	0.031	0.149	-20817.344
	Equation	$RCO_2 = \frac{(0.677).YO_2}{21.617+\left(1+\frac{YCO_2}{0{,}031}\right).YO_2}$	$RCO_2 = \frac{(4.044).YO_2}{27.065+\left(1+\frac{YCO_2}{0{,}149}\right).YO_2}$	$RCO_2 = \frac{(45.380).YO_2}{-0.041+\left(1+\frac{YCO_2}{-1094{,}205}\right).YO_2}$
Noncompetitive	α	-0.58242	-3.11443	42.76371
	φ	-20.5724	-24.3615	-0.12613
	γc	-3.493	-19.674	88.870
	Equation	$RCO_2 = \frac{(0.582).YO_2}{(YO_2-(20.572)).\left(1-\frac{YCO_2}{(3{,}493)}\right).}$	$RCO_2 = \frac{(-3.114).YO_2}{(YO_2-(-24.361)).\left(1-\frac{YCO_2}{(-19.674)}\right).}$	$RCO_2 = \frac{(42.764).YO_2}{(YO_2-(0.126)).\left(1-\frac{YCO_2}{(88.870)}\right).}$
Combination	α	-0.58242	-3.11443	42.76371
	φ	-20.5724	-24.3615	-0.12613
	γc	-4.19822	-12.8793	-30.3806
	γu	-3.49298	-19.6739	88.86987
	Equation	$RCO_2 = \frac{(-0{,}582).YO_2}{(-20.572).\left(1-\frac{YCO_2}{-4.198}\right)+YO_2\left(1-\frac{YCO_2}{(-3.492)}\right).}$	$RCO_2 = \frac{(-3.114).YO_2}{(-24.3615).\left(1-\frac{YCO_2}{-12.879}\right)+YO_2\left(1-\frac{YCO_2}{(-19.673)}\right).}$	$RCO_2 = \frac{(42.763).YO_2}{(-0.126).\left(1-\frac{YCO_2}{-30.380}\right)+YO_2\left(1-\frac{YCO_2}{(88.869)}\right).}$

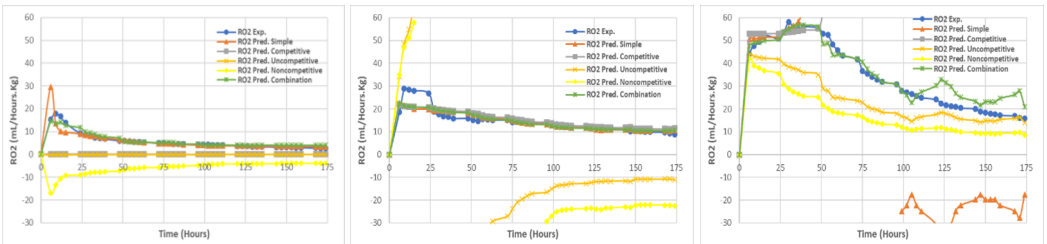

Fig. 5. Predicted Respiration Rates (RO_2) from the Michaelis–Menten Model for Samples at Different Storage Temperatures

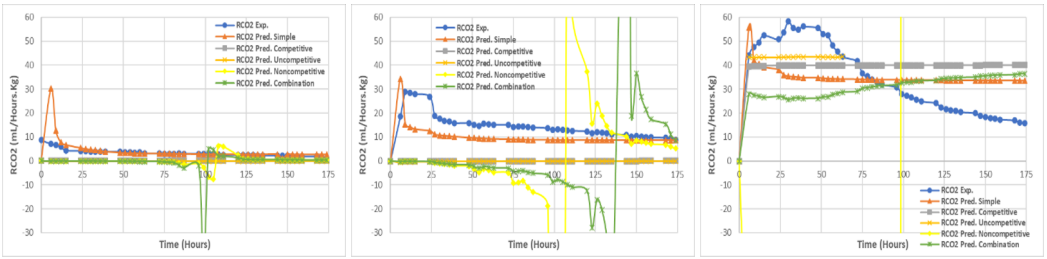

Fig. 6. Predicted Respiration Rates (RCO_2) from the Michaelis–Menten Model for Samples at Different Storage Temperatures

Table 7. Validation Test Results of Michaelis-Menten Respiration Rate Modeling

MM Model	Storage Temp. (°C)	RO_2				RCO_2			
		R^2	P *value* X^2	SSE	RMSE	R^2	P *value* X^2	SSE	RMSE
Simple	7	0.655	0.795	11.431	3.381	0.959	0.999	4.743	2.177
	17	0.712	0.999	5.457	2.336	0.586	0.991	9.369	3.060
	27	0.558	0.999	6.437	2.537	0.517	0.999	13.496	3.673
Competitive	7	0.898	0.001	112.59	10.611	0.556	0.001	83.606	9.143
	17	0.881	0.001	159.47	12.628	0.449	0.001	130.28	11.414
	27	0.818	0.001	427.80	20.683	0.214	0.979	18.507	4.302
Uncompetitive	7	0.709	0.001	105.04	10.248	0.882	0.001	83.181	9.120
	17	0.727	0.001	65.227	8.076	0.762	0.001	126.47	11.246
	27	0.668	0.027	66.166	8.256	0.213	0.001	211.67	14.549
Noncompetitive	7	0.694	0.001	85.107	9.225	0.595	0.001	83.141	9.118
	17	0.727	0.001	75.766	8.588	0.407	0.001	123.65	11.11
	27	0.374	0.001	449.06	21.191	0.409	0.001	440.05	20.977
Combination	7	0.860	0.999	2.924	1.710	0.940	0.999	1.233	1.110
	17	0.800	0.999	5.922	2.433	0.842	0.999	2.535	1.592
	27	0.988	0.999	0.486	0.697	0.505	0.999	6.195	2.489

The superior performance of the combined competitive–uncompetitive Michaelis–Menten model in this study can be attributed to the coexistence of dual inhibition mechanisms during banana storage. O_2 functions as the primary substrate in the respiratory process, while CO_2, the principal metabolic byproduct, accumulates over time and exerts an inhibitory effect on enzymatic activity. Specifically, CO_2 may compete with O_2 for the enzyme's active site (competitive inhibition) while simultaneously interacting with the enzyme–substrate complex, thereby diminishing catalytic efficiency (uncompetitive inhibition). Under storage conditions where O_2 concentration gradually decreases and CO_2 concentration increases, a single inhibition mechanism fails to adequately capture the complexity of respiration kinetics. Consequently, the combined model more accurately reflects the dynamic interplay between O_2 and CO_2, resulting in the best agreement with the experimental data across all treatments.

4 Conclusion

The results demonstrated that storage temperature had a significant effect on the respiration rate of Cavendish bananas, where higher temperatures accelerated the respiration process. The Arrhenius model effectively described the CO_2 respiration kinetics, as indicated by correlation coefficients (R^2) close to one and Chi-square (χ^2) p-values greater than 0.05. Meanwhile, the Michaelis–Menten modeling revealed that the combined competitive–uncompetitive inhibition type provided the best fit among all tested models. Validation

results supported this finding with high R^2 values, p-values above 0.05, and low SSE and RMSE values, confirming that the developed models achieved high predictive accuracy with minimal deviation from experimental data. Furthermore, the developed models can be applied to optimize the storage conditions of Cavendish bananas, not only through temperature regulation, but also by controlling the gas composition within the storage environment, such as in Modified Atmosphere Packaging (MAP) or Controlled Atmosphere Storage (CAS) systems. These approaches allow adjustment of the O_2 and CO_2 balance to suppress respiration rates in accordance with the combined Michaelis–Menten model that incorporates enzymatic inhibition mechanisms. Controlled accumulation of CO_2 can act as a natural inhibitor, reducing respiration activity without compromising fruit quality.

References

[1] FAO 2025 Banana Market Review - Preliminary Results 2024. Rome.
[2] Goldie K Vijaya R AB Waheed W Sanjeev K 2024 International Journal of Advanced Biochemistry Research 8 (5) 327 – 335
[3] Dimas T and N Bintoro. 2021. J Agrointek 15 452-458
[4] Rahman E A A. Talib R A. Aziz M G and Yusof Y A 2013 *Fruits Food Sci Biotechnol* **22** 1581–8
[5] Dwi R N Bintoro. AD Saputro 2021 J Agrointek 15 90 – 91
[6] Ho P L. Tran D T. Hertog M L A T M and Nicolaï B M 2020 Sci Hortic 263 109138
[7] Barbosa N C. Mendonça Vieira R A and de Resende E D 2018 Postharvest Biol Technol 136 152–60
[8] Zahrah-Izati A S Siti H A Rosnah S Intan S M A T Konstantinos G 2021 J Food Packaging and Shelf Life 28
[9] M J Pereira A. L. Amara M. Pintado M. F. Pocas 2025 J Postharvest Biology and Tech. 131 1 - 9
[10] Nayara C B Ricardo A M V Eder D R 2018 J Postharvest Biology and Tech. 136 152 - 160
[11] Johanna G Anibal O H Diego A Castellanos 2021 J Biosystem Engineering 208 152 - 163
[12] Phuc L. H Dinh T T Maarten L A T M H Bart M N 2020 J Scientia Horticulturae 263
[13] Manju J Hui X Annelies P Maarteen H Pieter V Bart N Wouter S 2024 J Postharvest Biology and Tech. 213
[14] M.J. Pereira A.L. Amaro M. Pintado M.F. Poças 2017 Postharvest Biology and Technology 131 1-9
[15] Brian J H Gregory H L Richard G L 2017 J Environ Sci Technol 51 (9) 5156 – 5164
[16] Komolafe C A Ojediran J O Ajao F O Dada O A Afolabi Y T Oluwaleye I O and Alake A S 2019 *Case Stud Therm Eng* **15** 100542
[17] Kader A A 2013 Journal of Applied Sciences and Technology 1(1) 1–8.
[18] Charalampos G T Georgios T X 2021 J Biosystem Engineering 232 129 - 140
[19] Agudelo C and Restrepo C 2016 *Rev Fac Na Agron* **69** 7985–95